PARAMETRIC MODELING OF HUMAN WRIST FOR BIOIMPEDANCE-BASED PHYSIOLOGICAL SENSING

Kaan Sel[1], Noah Huerta[2], Michael S. Sacks[5] and Roozbeh Jafari[3,4]

[1] Departments of Electrical and Computer Engineering, [2] Mechanical Engineering, [3] Biomedical Engineering, [4] Computer Science and Engineering, Texas A&M University, College Station, TX, US
[5]James T. Willerson Center for Cardiovascular Modeling and Simulation
The Oden Institute and the Department of Biomedical Engineering,
The University of Texas at Austin, Austin, TX, USA

ABSTRACT

Bioimpedance is a powerful modality to continuously and non-invasively monitor cardiovascular and respiratory health parameters through the wearable operation. However, for bioimpedance sensors to be utilized in medical-grade settings, the reliability and robustness of the system should be improved. Previous studies provide limited fundamental analyses of the factors involved in the system that impact the sensitivity and the specificity of the modality in capturing the hemodynamics. This study provides a parametric model of the human wrist that involves different tissue layers (i.e., skin, fat, artery, muscle, bone) with complex dielectric properties built based on the human wrist anatomy. We run a frequency domain electrical field simulation using finite element analysis to map electric current distribution within the wrist to find the optimum operating frequency and electrode placement that provide the highest sensitivity and specificity to the blood flow. Our results suggest using an operating frequency between 10-100 kHz range with minimal electrode separation to capture the pulsatile activity with high accuracy.

Index Terms— bioimpedance, blood flow, wrist modeling, COMSOL, physiological sensing

1. INTRODUCTION

Continuous monitoring of cardiovascular health parameters in both healthy and disordered individuals is essential to provide more effective prognostic and diagnostic services. This requires replacing invasive and bulky systems that mostly operate in hospital settings with opportunistic modalities that are non-invasive and allow wearable operation. One principal challenge, however, is the low sensitivity and specificity obtained from these non-invasive modalities in capturing the changes in the hemodynamic parameters, especially when implemented within a wearable form factor (*e.g.*, wrist-worn).

Bioimpedance is a promising method that depends on non-invasive excitation of the human skin with a high-frequency and small scale electric current to measure the changes in the underlying body tissue impedances. Bioimpedance measurements are non-invasive, low-cost, and support wearable operation. In addition, they provide high sensitivity to the arterial blood flow, when the sensors are placed across the wrist to provide complex hemodynamic (e.g., blood pressure [1], arterial compliance [2]) and respiratory parameters (*e.g.*, respiration rate [3]–[5]). However, the changes in the bioimpedance signal can be due to other factors (*e.g.*, muscle contractions, motion, body fluid shifts and composition changes). Therefore, the specificity of the bioimpedance sensing to the blood flow should be improved to provide reliable hemodynamic monitoring for the modality to translate from research level investigations to medical grade applications.

There are multiple studies that test bioimpedance as a tool in measuring cardiovascular health through an extensive experimental analysis. However, the fundamental understanding of the human body response to the electrical stimulation is still not well established. The distribution of the electric current under different injection electrode placements and the effect of injection frequency to the penetration depth is unknown. There are recent studies that model the human wrist to provide a fundamental analysis of the bioimpedance modality. However, these studies either do not investigate the bioimpedance changes specifically due to the arterial blood flow [6], or do not explore the distribution of the current within the different tissue types under different electrode separations and injection frequencies [7], or provide a preliminary assessments of the electric field distribution in simplified two-dimensional models with limited analysis on the sensitivity to the cardiac activities [8]. Hence, there is an unmet need to study a human body/tissue model that would provide a mapping of the electrical current within the human body to localize the blood flow in bioimpedance sensing to improve both the specificity and the sensitivity of the modality in cardiac event monitoring.

In this paper, we introduce a three-dimensional (3-D) parametric human wrist model with frequency dependent properties defined for the underlying skin, arteries, fat, and muscle tissues to analyze the vector distribution of the electric current using finite element analysis (FEM). Our contributions in this paper can be summarized as follows:

- Introducing a 3-D frequency-dependent parametric human wrist model with multiple tissue layers (*i.e.*, skin, fat,

artery, muscle, and bone) to investigate the distribution and penetration of the electrical current.

- Presenting an exploration of the effects of parameters involved in bioimpedance sensing (*i.e.*, sensor placement and operational frequency) to maximize the current distribution in the artery.
- Proposing a sensitivity measurement of bioimpedance to locate an arterial pulse and provide a cross-validation of the analysis with the current distribution analysis.

2. MATERIALS AND METHODS

2.1 Three-dimensional human wrist model

We built a 3-D parametric model of the human wrist using COMSOL Multiphysics 5.5. The model consists of different tissue layers (i.e., skin, fat, artery, muscle, and bone) to replicate the human anatomy, as shown in Figure 1. We used complex permittivity and conductivity values for different tissue layers to obtain frequency dependent dielectric properties through a definition of Cole-Cole model parameters [9]. The skin layer is composed of the more conductive living epidermis and dermis, with a total of 1.1 mm thickness [10]. To account for the thin stratum corneum layer, we added a constant per unit area contact resistance and capacitance of 34.9 kΩ/cm^2 and 4.6 nF/cm^2, respectively at the skin-electrode boundary [11]. We defined a fat layer under the skin with 6 mm thickness [10], followed by a 7 mm thick muscle layer [8] circulating 10 mm thick bone layer [8]. The wrist contains two arteries, namely the radial and ulnar arteries, that carry oxygenated blood with the necessary nutrients to the tissues. In our model to simplify the anatomical complex structure, we situated the two arteries in parallel to each other and 3 mm under the skin, buried within the fat layer, on two sides of the model [12]. The arteries measure 2.6 mm in internal diameter with a wall thickness of 0.2 mm [13] and span the full 10 cm length (at least two times larger than the area of interest) to obtain continuity in the simulations and avoid the boundary effects.

We placed four 5 mm by 5 mm silver electrodes uniaxially over the main artery with equal spacing between each electrode. We used the COMSOL AC/DC Module to define the outer two electrodes as terminals for current injection (left outer electrode) and ground (right outer electrode). The two inner electrodes provide voltage readings through a defined voltage probes as a part of the 4-terminal sensing (Kelvin sensing). We used default COMSOL physics-controlled meshing with finer resolution to run FEM. We defined a frequency domain study to determine the current density distribution in the wrist at a defined operating frequency and electrode placement.

2.2 Analysis of the current density in the arteries

The AC/DC simulation results provide the distribution of the electric current density components (J_x, J_y, J_z) for all three axes over the entire model, with the coordinate orientation shown in Figure 1. The model is centered at the equal distance to the outer

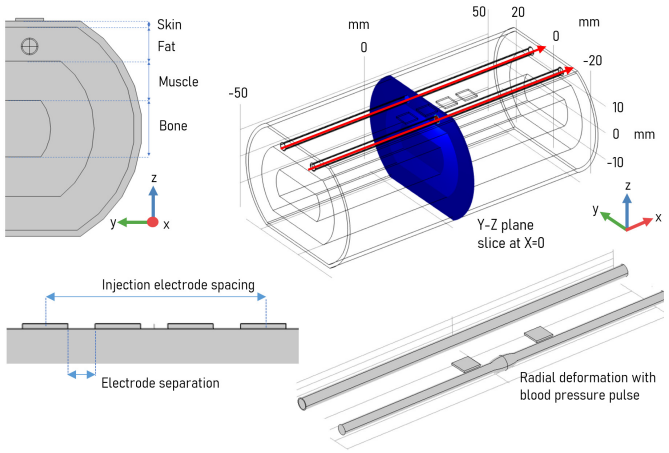

Fig. 1. Proposed parametric human wrist model.

(and inner) electrodes. Here, J_x component of the current density measures the current flow towards the *X*-axis (towards the ground electrode, alongside the artery). Therefore, to capture the total current flowing through each artery a surface integral should be calculated across the artery surface as shown below.

$$\oiint_{S:artery} J_x \cdot \overrightarrow{dS} \tag{1}$$

Here J_x is the *X* component of the current density and $\overrightarrow{dS}$ is the differential surface area element in *Y-Z* plane that vertically cuts the wrist, and the surface is defined separately from the surface areas of main and secondary arteries. Note that the surface integral of the full surface area yields the total amount of current that is injected into the tissue. Therefore, calculation of the current flow in the artery does not require a scaling for different simulation configurations as long as the injected current is kept constant. For all operating frequency points and different electrode calculations, the surface integral shared in (1) is calculated in MATLAB for the *Y-Z* plane sliced at the center of the *X*-axis (i.e., $X = 0$), as shown in Figure 1.

In addition to the sliced surface, we exported the simulation data for the two lines that are passing through the center of the main and secondary arteries to extract the distribution of the current density alongside the artery. We analyzed the line data to obtain the maximum value of the current density across the artery for each configuration to understand the effect of frequency and electrode placement in the current penetration, and to comment on the contribution of the secondary artery to the bioimpedance causing a low accuracy in pulse optimization traveling in the main artery.

2.3 Pulse design and sensitivity simulations

In addition to the current distribution analyses, we tested the change in the bioimpedance measured in terms of the change in the differential voltage across the inner voltage sensing

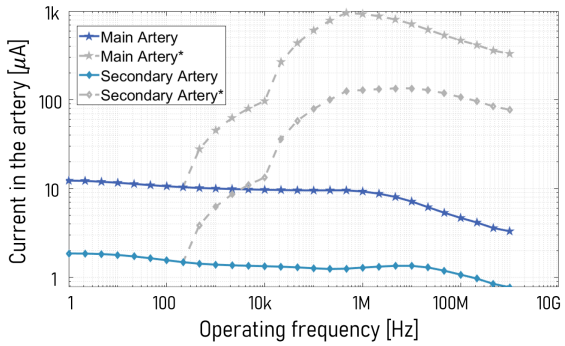

Fig. 2. Total current flowing through the arteries at different frequencies, under 0.1 mA excitation, at the artery center. The gray plots show the estimated current amplitudes in case the injected current is increased based on the safety standards.

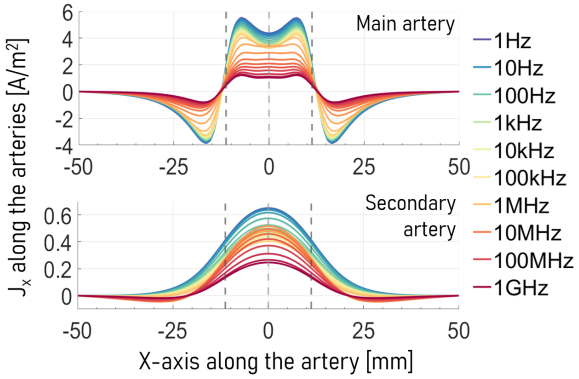

Fig. 3. X-component of the current density extracted at the lines along the arteries.

electrodes in the presence of a blood pressure pulse in the main artery. Therefore, for this analysis, we placed a pulse at the center of the two sensing electrodes and introduced a radial deformation of 1.5 mm [14], as shown in Figure 1.

3. RESULTS AND DISCUSSION

3.1 Assessment of the effect of frequency on current distribution across arteries

There are two main frequency dependent factors that limit the amount of current injected to the skin in bioimpedance sensing: 1) the high voltage drop across the injection electrodes due to high electrode-skin impedance that is usually dominant at lower frequencies (<100 Hz), forcing the bioimpedance sensing to happen at frequencies higher than 1 kHz [15], 2) the electrical safety standards that limit the current to be: i) 0.1 mA when frequency is less than 1 kHz, ii) linearly increasing from 0.1 mA till 10 mA when a logarithmic increase in frequency from 1 kHz to 100 kHz, iii) 10 mA at frequencies higher than 100 kHz [16]. In our simulations we used a constant injection of 0.1 mA across two square-shaped metal electrodes to test a realistic amplitude

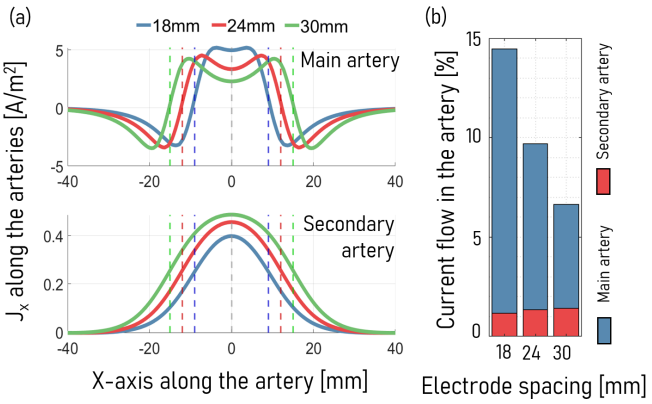

Fig. 4. Impact of injection electrode spacing to the overall current distribution. (a) J_x component of the current density, (b) total current flowing through the arteries.

for the current, with 24 mm spacing between the injection electrodes. We held a frequency sweep on the wrist model from 1 Hz to 1 GHz, with 3 frequency points each decade to analyze the association of the operation frequency and the current distribution over the wrist. Figure 2 shows the amount of current that flows within the main and the secondary arteries measured at the center of the model through a surface integral of the J_x slice extracted at the model center. In addition, the plot includes the expected values of the current flow in the arteries with an increase in the injection amplitude considering the limits determined by the safety standards. We observe that although the current amplitude gradually decreases with increasing frequency, higher frequency regions dominates the low frequency due to increased safety limits for the current injection. Therefore, increasing the injection frequency till 1 MHz yields a higher sensitivity to the blood flow due to the allowance of orders of magnitude of increased current injection amplitude with increasing frequency.

The analysis of the J_x component of the current measured at the line drawn in the middle of the arteries is shown in Figure 3. We observe a similar trend in terms of the maximum current density levels for different frequencies, where increasing frequency till 1 MHz yields a higher sensitivity to the blood flow, since the decrease in the current amplitude is significantly less than the increase in the limits of injection determined by the safety standards. We observe no change in both the spatial location of the maximum current density and the zero-crossing level that marks the entrance of the current to the arteries for different operating frequencies.

3.2 Assessment of the effect of injection electrode spacing on current distribution across arteries

In order to find the impact of electrode separation on the sensitivity and specificity of bioimpedance measurement to the arterial blood flow, we simulate the model under three different spacing between the injection electrodes (*i.e.*, center-to-center spacing: 18 mm, 24 mm, 30 mm). Figure 4(b) shows the surface

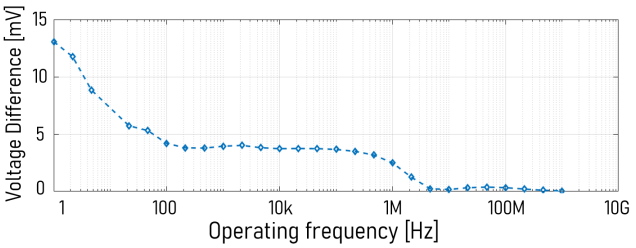

Fig 5. The change in voltage due to pulse presence under different operating frequencies

integral of the electric current density that measures the total current flow across the main and secondary arteries measured at the center of the model (*i.e.*, X = 0). We observe that the higher separation between injection electrodes decreases the amount of current flowing through the main artery due to higher leakage of the current towards the neighboring tissues. On the other hand, we observe a reverse trend in the secondary artery where higher spacing between the injection electrodes leads to a higher current flow in the secondary arteries. This is in agreement with our justification for the decrease in the total current flow in the main artery with increased spacing, where higher separation allows the current to flow in neighboring tissues, hence leads to a higher current accumulation at the secondary wrist artery. Figure 4(a) shows a similar pattern for the J_x component of the current density measured across the arterial line for both arteries, where while the main artery receives a lesser amount of current flow with the increased spacing, the secondary artery has a higher current flow in return. In addition, as expected, the higher spacing between the injection electrodes leads the current to flow within the arteries for longer distances (*i.e.*, the effective distance is higher).

The results suggest that the higher spacing decreases both the sensitivity and the specificity of bioimpedance measurement in capturing arterial blood flow since; 1) lesser current flows in the main artery leading to a decrease in sensitivity, 2) higher current flows in the secondary artery leading to an error in the localization of the pulse traveling in the main artery. For measurements, such as in pulse-transit time (PTT), where the localization of the pulse is essential for successful operation [17], our results suggest the use of lower separation between the injection electrodes due to higher specificity and sensitivity, and smaller effective distance that yields a better localization.

3.3 Blood pressure pulse localization

In order to measure the relative changes in the bioimpedance signal due to the appearance of a blood pressure pulse, we used the four-probe sensing method to capture the bioimpedance. Here, the outer electrodes were used for current injection and the inner electrodes were used for the voltage sensing due to bioimpedance. To compare the sensitivity of bioimpedance to the blood flow, we defined an artificial pulse at the center of the artery, as shown in Figure 1. We recorded the change in the voltage difference measured across the inner electrodes (ΔV_{bioz}) due to the inclusion of the pulse at different operating frequencies and electrode spacings. Figure 5 shows ΔV_{bioz} at different operating frequencies. We observe a decrease in the sensitivity with increasing frequency up to 100 Hz. However, bioimpedance sensing is not applicable at low frequency range due to impractically high levels of electrode-skin impedance. From 100 Hz till 100 kHz, we observe a plateau in ΔV measurements, where increasing the frequency above 100 kHz causes a decrease in the measured ΔV. These findings are in line with the arterial current distribution analysis and suggest the usage of a frequency range of 10 - 100 kHz for bioimpedance measurements sensitive to pulsatile activity. Moreover, to find the optimum electrode separation between the electrodes that yields the highest ΔV_{bioz}, we tested three different configurations (*i.e.,* electrode separations, 1 mm, 3mm, 5mm). We obtained the highest voltage difference for 1 mm separation (ΔV_{bioz} measured for 1 mm, 3 mm and 5 mm separations: 398 mV, 61 mV, and 38 mV respectively) in agreement with the current density analysis with different electrode spacings, suggesting the usage of minimal separation between the injection and sensing electrodes to obtain higher sensitive pulse monitoring.

4. CONCLUSION

In this paper, we introduce a parametric bioimpedance model that is built based on the human wrist anatomy to analyze the electrical current distribution after the stimulation of the skin with a current source. The model consists of different tissue layers with frequency dependent dielectric properties to investigate the impact of the operating frequency and the spatial placement of the electrodes to the sensitivity and specificity of the bioimpedances in capturing the blood flow. The results suggest an optimal frequency range for bioimpedance applications with minimal electrode spacing. We purposely selected the dimensions and placement for each tissue layer, with the specific focus on the radial and ulnar arteries. Nevertheless, in future, we are planning to extend our framework to use a more realistic human wrist model incorporating unique shapes and dimensions of muscles, tendons, bones, and other tissue layers, and realistic arterial mechanical behaviors. In addition, we are planning to run experimental validation for the simulation results to further justify the outcomes of this study. We believe that, the proposed model has the potential to provide further investigations related to bioimpedance sensing (e.g., current penetration with different body fat ratios) that are essential for the modality to be used in practical settings.

5. ACKNOWLEDGMENT

This work was supported in part by the National Institutes of Health under grant 1R01HL151240. Any opinions, findings, conclusions, or recommendations expressed in this material are those of the authors and do not necessarily reflect the views of the funding organizations.

6. REFERENCES

[1] B. Ibrahim and R. Jafari, "Continuous Blood Pressure Monitoring using Wrist-worn Bio-impedance Sensors with Wet Electrodes," in *2018 IEEE Biomedical Circuits and Systems Conference (BioCAS)*, 2018, pp. 1–4.

[2] R. Ben Salah, T. Alhadidi, I. Ben Salah, and K. Ouni, "Non-invasive determination of the arterial compliance by cardiovascular bioimpedance signal processing," in *2018 IEEE 20th International Conference on e-Health Networking, Applications and Services (Healthcom)*, 2018, pp. 1–6.

[3] K. Sel, D. Osman, and R. Jafari, "Non-Invasive Cardiac and Respiratory Activity Assessment From Various Human Body Locations Using Bioimpedance," *IEEE Open J. Eng. Med. Biol.*, vol. 2, pp. 210–217, Jun. 2021.

[4] K. Sel, A. Brown, H. Jang, H. M. Krumholz, N. Lu, and R. Jafari, "A Wrist-worn Respiration Monitoring Device using Bio-Impedance," in *Proceedings of the Annual International Conference of the IEEE Engineering in Medicine and Biology Society, EMBS*, 2020, vol. 2020-July, pp. 3989–3993.

[5] K. Sel, B. Ibrahim, and R. Jafari, "ImpediBands: Body Coupled Bio-Impedance Patches for Physiological Sensing Proof of Concept," *IEEE Trans. Biomed. Circuits Syst.*, vol. 14, no. 4, pp. 757–774, Aug. 2020.

[6] G. Anand, A. Lowe, and A. M. Al-Jumaily, "Simulation of impedance measurements at human forearm within 1 kHz to 2 MHz," *J. Electr. Bioimpedance*, vol. 7, no. 1, pp. 20–27, 2016.

[7] K. Pesti, M. Metshein, P. Annus, H. Kõiv, and M. Min, "Electrode placement strategies for the measurement of radial artery bioimpedance: Simulations and experiments," *IEEE Trans. Instrum. Meas.*, vol. 70, pp. 1–10, 2020.

[8] R. Abdelbaset, M. El Dosoky, and M. T. El-Wakad, "The effect of heart pulsatile on the measurement of artery bioimpedance," *J. Electr. Bioimpedance*, vol. 8, no. 1, pp. 101–106, 2017.

[9] C. Gabriel, "Compilation of the dielectric properties of body tissues at RF and microwave frequencies.," 1996.

[10] K. Hwang, H. Kim, and D. J. Kim, "Thickness of skin and subcutaneous tissue of the free flap donor sites: a histologic study," *Microsurgery*, vol. 36, no. 1, pp. 54–58, 2016.

[11] R. Pethig, "Dielectric properties of body tissues," *Clin. Phys. Physiol. Meas.*, vol. 8, no. 4A, p. 5, 1987.

[12] J. S. Roberts and R. Manur, "Ultrasound-guided radial artery access," *Card. Interv. Today*, pp. 39–43, 2013.

[13] S. Beniwal, K. Bhargava, and S. K. Kausik, "Size of distal radial and distal ulnar arteries in adults of southern Rajasthan and their implications for percutaneous coronary interventions," *Indian Heart J.*, vol. 66, no. 5, pp. 506–509, Sep. 2014.

[14] P. Choudhari and M. S. Panse, "Finite element modeling and simulation of arteries in the human arm to study the aortic pulse wave propagation," *Procedia Comput. Sci.*, vol. 93, pp. 721–727, 2016.

[15] K. Sel, D. Kireev, A. Brown, B. Ibrahim, D. Akinwande, and R. Jafari, "Electrical Characterization of Graphene-based e-Tattoos for Bio-Impedance-based Physiological Sensing," in *BioCAS 2019 - Biomedical Circuits and Systems Conference, Proceedings*, 2019.

[16] *Medical electrical equipment Part 1: General requirements for basic safety and essential performance ANSI/AAMI ES60601-1:2005/A1:2012*. .

[17] B. Ibrahim, A. Akbari, and R. Jafari, "A novel method for pulse transit time estimation using wrist bio-impedance sensing based on a regression model," in *Biomedical Circuits and Systems Conference (BioCAS), 2017 IEEE*, 2017, pp. 1–4.